ISSN 0025-6544, Mechanics of Solids, 2015, Vol. 50, No. 5, pp. 546–558. © Allerton Press, Inc., 2015.
Original Russian Text © N.G. Burago, I.S. Nikitin, P.A. Yushkovskii, 2015, published in Izvestiya Akademii Nauk. Mekhanika Tverdogo Tela, 2015, No. 5, pp. 78–93.

Lifetime of Disks of Variable Thickness with Anisotropy of Fatigue Properties Taken into Account

N. G. Burago[1,2*], I. S. Nikitin[2,3], and P. A. Yushkovskii[4]**

[1] *A. Ishlinsky Institute for Problems in Mechanics, Russian Academy of Sciences, pr. Vernadskogo 101, str. 1, Moscow, 119526 Russia*
[2] *Bauman Moscow State Technical University, ul. 2-ya Baumanskaya 5, Moscow, 105005 Russia*
[3] *Institute of Design Automation, Russian Academy of Sciences, ul. 2-ya Bratskaya 19/18, Moscow, 123056 Russia*
[4] *MATI — K. E. Tsiolkovsky Russian State Technological University, ul. Orshanskaya 3, Moscow, 121552 Russia*

Received February 27, 2014

Abstract—A generalization of well-known criteria for multiaxial fatigue fracture to the case of titanium alloys with anisotropic fatigue properties is proposed. The problem of determining the stress-strain state and estimating the fatigue life of a rotating disk of variable thickness under the action of centrifugal loads in the disk and blades is solved. The proposed criteria for multiaxial fatigue fracture are used to obtain spatial lifetime distributions over the disk in the isotropic and anisotropic cases. It was shown that the fatigue life of the titanium disk with the anisotropy of the fatigue properties taken into account can decrease to the critical values of N, 10^4 cycles near the outer rim of the disk in the region of contact with blades, which is inadmissible from the standpoint of safe operation.

DOI: 10.3103/S0025654415050064

Keywords: *fatigue fracture, anisotropy, fatigue life, compressor disk, centrifugal load, aerodynamic pressure.*

1. INTRODUCTION

The disk of the aircraft compressor of a gas-turbine engine is a complex technical object of strongly varying thickness with overflow and balance holes, which are stress concentrators. The stress-strain states of such a disk can be computed only by modern software complexes on the basis of finite-element methods. For example, such computations were earlier performed in [1–2].

The main goal in this paper is to estimate how the anisotropy of the fatigue properties of titanium alloy affects the lifetime of the compressor disk in a gas-turbine engine in the low-cycle loading mode (takeoff–flight–landing). In the process of cyclic loading, the disk operates within the elasticity margin, and to apply the fatigue strength criterion, one needs to determine the range of variations in the stress-strain state due to the action of centrifugal loads as well as contact loads exerted by the blades, which, in turn, are subjected to centrifugal and aerodynamic loads.

In the present paper, the well-known Sines–Crossland criteria [3–4] for isotropic materials are generalized to the case of titanium alloys with anisotropic properties. A procedure is developed for determining the parameters of the generalized criteria from the results of uniaxial fatigue tests in the direction of axes having various orientation with respect to a distinguished direction of the ally texture. We choose the Sines–Crossland models as a basis for constructing generalized criteria because these models are classical nowadays and agree well with the Hill methodology [10] accepted in the theory of plasticity for its generalization to the anisotropic case. The new approach based on the concept of critical

* e-mail: burago@ipmnet.ru
** e-mail: i_nikitin@list.ru

plane [5–7], for example, the well-known Findley criterion [8], along with the Sines–Crossland criteria, has already been used by the authors [9] to estimate the fatigue life.

We note that, in the real operation, the structural anisotropy due to the technological processes of half-finished material manufacture is superimposed on the constructional anisotropy due to the accumulation of fatigue damage [11–13]. In this paper, we consider only the influence of structural anisotropy, but the influence of construction anisotropy and, so much the more, the the complex influence of these two types of anisotropy are beyond the scope of this study and deserve special analysis.

In the considered low-cyclic fatigue mode, the cyclic actions correspond to the flight loading cycles (takeoff–flight–landing). The actual flight cycle has a multistage character with unsteady processes at each of the stages. In the present paper, we assume that the cyclic loading process is harmonic.

Simplifying hypotheses about the dependence of the solution on the coordinates across the disk thickness and in the circular direction were used to derive a system of ordinary differential equations for computing the radial stress, strain, and displacement distributions in a disk of small but variable thickness. A numerical scheme for solving the obtained rigid system of ordinary differential equations is proposed and implemented. Thus, the well-known analytic method for the analysis of axisymmetric loaded disks [14] is generalized to the case of nonaxisymmetric loading, which can be of interest in itself.

The additional stresses in the rim part of the disk due to the blade bending under the action of aerodynamic pressures are also taken into account. The aerodynamic pressures are determined on the basis of the "isolated profile" hypothesis by using the known solutions of the problem on the flow with separation past a plate. The computed stress-strain state and generalized criteria for multiaxial fatigue fracture in the isotropic and anisotropic cases are used to obtain the lifetime distribution over the disk, The dangerous regions and the fatigue lifetimes are determined in the disk.

It is shown that fatigue life of a titanium disk with anisotropy of the fatigue properties taken into account can decrease to the critical values $N \sim 10^4$ of flight cycles near the inner and outer disk rims, which is inadmissible from the standpoint of safe operation and requires changes in the disk production technology to increase the fatigue limit in the near-surface layer.

2. CRITERIA OF MULTIAXIAL FATIGUE FRACTURE WITH ANISOTROPY OF THE FATIGUE PROPERTIES OF TITANIUM ALLOY TAKEN INTO ACCOUNT

Influence of the Anisotropy of the Fatigue Properties of Titanium Alloy on Uniaxial Fatigue Curves

Earlier, in [1, 2, 15], the stress-strain state and the fatigue life of titanium disks of gas-turbine engine disks was already studied in flight loading cycles. To this end, a method for determining the parameters of isotropic multilayer criteria for fatigue fracture [16] was proposed on the basis of the results of uniaxial tests for various coefficients of the cycle asymmetry. In that paper, FEM computations were used to determine the regions of fatigue microcrack origination near the rim part of the disk. In the exploitation of this structure element, fracture also occurs in the near-surface region [17] but somewhat closer to the central part of the disk. To refine the computed location of such region, it was conjectured that such a displacement can be caused by the anisotropy of of the titanium alloy properties due to the texture induced in the technological processes of half-finished material manufacturing (mainly, in rolling). In the present paper, a specific example is used to estimate the influence of structural anisotropy of the material fatigue properties on the location of the damage origination region and the disk lifetime in the case of low-cycle fatigue.

The effect of fatigue limit dependence on the loading axis direction in uniaxial fatigue tests of specimens with texture was noted in various sources [18, 20]. In [20], one can find the results of the corresponding fatigue tests, which are illustrated in Fig. 1, and data on the dependence of strength and fatigue characteristics of titanium alloy Ti-6Al-4V on the texture orientation with respect to the loading direction. (In Fig. 1, black disks correspond to the case where the orientation axis is parallel to the loading axis; black squares correspond to the case where the orientation axis is perpendicular to loading axis; the stresses are measured in kgf/mm^2.)

A generalization of the multiaxial fatigue criterion on the basis of the equation for Lemaitre–Chaboche-type damage to the case of alloys with anisotropy of the fatigue properties was proposed in [21, 22]. This generalization is based on the change of the second invariant of the stress deviator by the Hill function proposed in [10] to describe the anisotropic plasticity of metals,

$$\Sigma_{\text{Hill}} = \sqrt{H(\sigma_{11}-\sigma_{22})^2 + G(\sigma_{11}-\sigma_{33})^2 + F(\sigma_{22}-\sigma_{33})^2 + 2N\sigma_{12}^2 + 2L\sigma_{13}^2 + 2M\sigma_{23}^2}.$$

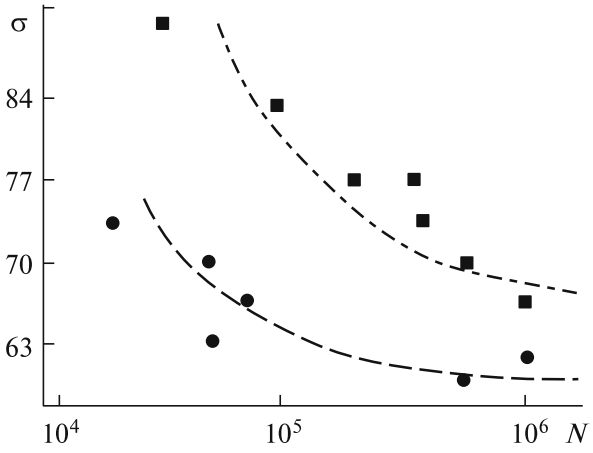

Fig. 1.

In [22], one can also find the Hill function parameters F, G, H, L, M, and N for the titanium alloy Ti-6Al-4V, which were determined from uniaxial fatigue tests along and across the rolling direction.

In the present paper, the idea of this change underlies the generalization of the classical Sines–Crossland criteria to the anisotropic case. A procedure for determining the parameters of fatigue fracture criteria was proposed in [16], and it was applied there to the criteria for isotropic materials. In what follows, we consider an application of this procedure to the fatigue criteria for anisotropic materials. To unify the form of isotropic and anisotropic criteria, instead of the Hill function, we introduce the equivalent Hill stress related to it by the formula

$$\tau_{\text{Hill}} = \frac{1}{3}\sqrt{(\sigma_{11}-\sigma_{22})^2 + \tilde{G}(\sigma_{11}-\sigma_{33})^2 + \tilde{F}(\sigma_{22}-\sigma_{33})^2 + 2\tilde{N}\sigma_{12}^2 + 2\tilde{L}\sigma_{13}^2 + 2\tilde{M}\sigma_{23}^2},$$

where $\tilde{G} = G/H$, $\tilde{F} = F/H$, $\tilde{N} = N/H$, $\tilde{M} = M/H$, and $\tilde{L} = L/H$.

Sines Model. Isotropic Criterion

According to [3], the generalization of the uniaxial fatigue criterion to the case of multiaxial stress state has the form

$$\frac{\Delta\tau}{2} + \alpha_s\sigma_{\text{mean}} = S_0 + AN^\beta, \quad \sigma_{\text{mean}} = (\sigma_1+\sigma_2+\sigma_3)_{\text{mean}},$$

$$\Delta\tau = \frac{1}{3}\sqrt{(\Delta\sigma_{11}-\Delta\sigma_{22})^2 + (\Delta\sigma_{11}-\Delta\sigma_{33})^2 + (\Delta\sigma_{22}-\Delta\sigma_{33})^2 + 6\Delta\sigma_{12}^2 + 6\Delta\sigma_{13}^2 + 6\Delta\sigma_{23}^2},$$

where σ_{mean} is the sum of principal stresses averaged over a loading cycle, $\Delta\tau$ is the variation in the octahedral tangential stress per cycle, $\Delta\tau/2$ is its amplitude, and α_s, S_0, A, and β are parameters determined from experimental data.

The procedure for determining the parameters of the multiaxial criteria from the results of uniaxial experiments with various cycle asymmetry coefficients is described in detail in [16]. In the isotropic case, the Sines criterion parameters have the form

$$S_0 = \frac{\sqrt{2}\sigma_{\text{u}}}{3}, \quad A = 10^{-3\beta}\frac{\sqrt{2}(\sigma_{\text{B}}-\sigma_{\text{u}})}{3}, \quad \alpha_s = \frac{\sqrt{2}(2k_{-1}-1)}{3}, \quad k_{-1} = \frac{\sigma_{\text{u}}}{3\sigma_{\text{u0}}},$$

where σ_{u} and σ_{u0} are the fatigue limits according to the fatigue curves with the cycle asymmetry coefficients $R = -1$ and $R = 0$, respectively, and σ_{B} is the ultimate strength.

Anisotropic Sines Criterion

The generalization of the Sines criterion to the anisotropic case with the above-described change has the form

$$\frac{\Delta\tau_{\text{Hill}}}{2} + \alpha_s\sigma_{\text{mean}} = S_0 + AN^\beta,$$

$$\Delta\tau_{\text{Hill}}=\frac{1}{3}\sqrt{(\Delta\sigma_{11}-\Delta\sigma_{22})^2+\tilde{G}(\Delta\sigma_{11}-\Delta\sigma_{33})^2+\tilde{F}(\Delta\sigma_{22}-\Delta\sigma_{33})^2+2\tilde{N}\Delta\sigma_{12}^2+2\tilde{L}\Delta\sigma_{13}^2+2\tilde{M}\Delta\sigma_{23}^2},$$

where $\tilde{G}=G/H$, $\tilde{F}=F/H$, $\tilde{N}=N/H$, $\tilde{M}=M/H$, and $\tilde{L}=L/H$.

By computing the parameters of the generalized criterion according to the scheme given in [16], we obtain

$$S_0=\frac{\sqrt{1+\tilde{G}}\sigma_{\text{u}}}{3},\quad A=\frac{10^{-3\beta}\sqrt{1+\tilde{G}}(\sigma_{\text{B}}-\Sigma_{\text{u}})}{3},\quad \alpha_s=\frac{\sqrt{1+\tilde{G}}(2k_{-1}-1)}{3}.$$

Crossland Model. Isotropic Criterion

In this case, according to [4], the generalization of the uniaxial fatigue curve to the case of multiaxial stress state has the form

$$\frac{\Delta\tau}{2}+\alpha_c\left(\bar{\sigma}_{\max}-\frac{\Delta\tau}{2}\right)=S_0+AN^{\beta},\quad \bar{\sigma}_{\max}=(\sigma_1+\sigma_2+\sigma_3)_{\max},$$

where $\bar{\sigma}_{\max}$ is the maximum sum of principal stresses over the loading cycle and the parameters α_c, S_0, A, and β are to be determined. In the isotropic case, the Crossland criterion parameters are given in [16],

$$S_0=\sigma_{\text{u}}\left[\frac{\sqrt{2}}{3}+\left(1-\frac{\sqrt{2}}{3}\right)\alpha_c\right],\quad A=10^{-3b}\left[\frac{\sqrt{2}}{3}-\left(1-\frac{\sqrt{2}}{3}\right)\alpha_c\right](\sigma_{\text{B}}-\sigma_{\text{u}}),$$

$$\alpha_c=\frac{k_{-1}\sqrt{2}/3-\sqrt{2}/6}{(1-\sqrt{2}/6)-k_{-1}(1-\sqrt{2}/3)}.$$

Anisotropic Crossland Criterion

By replacing the octahedral stress by the equivalent Hill stress, one obtains the generalized Crossland criterion

$$\frac{\Delta\tau_{\text{Hill}}}{2}+\alpha_c\left(\bar{\sigma}_{\max}-\frac{\Delta\tau_{\text{Hill}}}{2}\right)=S_0+AN^{\beta}.$$

By computing the parameters according to the scheme given in [16], we obtain

$$\alpha_c=\frac{k_{-1}\sqrt{1+\tilde{G}}/3-\sqrt{1+\tilde{G}}/6}{(1-\sqrt{1+\tilde{G}}/6)-k_{-1}(1-\sqrt{1+\tilde{G}}/3)},$$

$$S_0=\sigma_{\text{u}}\left[\frac{\sqrt{1+\tilde{G}}}{3}+\left(1-\frac{\sqrt{1+\tilde{G}}}{3}\right)\alpha_c\right],$$

$$A=10^{-3b}\left[\frac{\sqrt{1+\tilde{G}}}{3}+\left(1-\frac{\sqrt{1+\tilde{G}}}{3}\right)\alpha_c\right](\sigma_{\text{B}}-\sigma_{\text{u}}).$$

As a specific example that will be considered below, we present the following approximate values of the parameters for the titanium alloy Ti-6Al-4V [16, 21, 22]: the ultimate strength is $\sigma_{\text{B}}=1100$ MPa, the fatigue limits according to the amplitude fatigue curve with the symmetry coefficients $R=-1$ and $R=0$ are $\sigma_{\text{u}}=450$ MPa and $\sigma_{\text{u0}}=350$ MPa, respectively, the exponent in the polynomial dependence on the number of cycles is $\beta=-0.45$, the Young modulus is $E=116$ GPa, the shear modulus is $G=44$ GPa, and Poisson's ratio is $\nu=0.32$. The values of the Hill parameters for the titanium alloy with anisotropic fatigue properties are as follows [22]: $F=0.54$, $G=0.34$, $H=0.65$, and $N=M=L=2.34$.

3. DETERMINATION OF ADDITIONAL AERODYNAMIC LOAD ON THE DISK BLADES AND THE INFLUENCE ON THE DISK STRESS-STRAIN STATE

The computation of stress-strain state of rotating disks of a gas-turbine aircraft engine is a necessary stage of their fatigue strength and life estimation. As their operation experience shows, the region of possible fracture origination is located near the region of contact between the disk rim and the

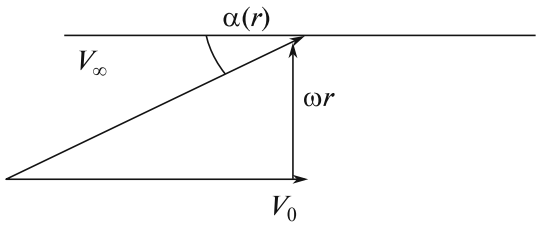

Fig. 2.

blade [16, 17]. The centrifugal forces are the main force factor in the light cycles of the disk-blade system loading. A vast literature is devoted to calculations of such actions on the disk. This problem has been solved by analytic and numerical-analytic method of the theory of elasticity and strength of materials [23–25] and contemporary program tools based on the finite element method [1, 2 15, 16]. But the aerodynamic loads arising in the flow of compressible gas (air) past the blades can be an additional factor affecting the disk stress-strain state in the region of its contact with blades. These aerodynamic loads cause additional strains in the blades, namely, bending and torsion strains. In this section, we estimate the additional stresses due to these strains at the blade root or, which is the same, on the outer rim of the disk under the blade, and compare them with the amplitude of the main stress field due to the centrifugal loads. For the blade, we use the model of clamped plate without initial twist taken into account.

Description of the Picture of Flow Past a Plate without and with the Flow Separation

The picture of flow past the cross-section of the compressor blade is shown in Fig. 2. We accept the "isolated profile" [27] hypothesis and use the following notation: r is the radial coordinate of the compressor blade cross-section, r_1 is the distance from the disk center to the blade root, r_2 is the distance from the disk center to the blade vertex, d is the width of the blade cross-section, V_0 is the velocity of the incoming flow, ω is the angular velocity of the blade rotation, and c is the speed of sound.

The presence of the "lattice" of blades is not taken into account, because in this case there is no foreseeable analytic solution of the problem on the flow with separation past the blades.

Figure 2 shows that the variable angle of incidence on the blade cross-section and the local speed are equal to $\alpha = \arctan(\omega r/V_0)$ and $V_\infty = \sqrt{V_0^2 + \omega^2 r^2}$.

For the flow without separation, the pressure difference on the cross-section and the displacement of the point of pressure application (focus) from the blade center [28] are determined by the formulas $\Delta p_b = \pi \rho V_\infty^2 d \sin\alpha \cos\alpha$ and $\bar{x}_b = d/4$.

For the separated flow, the pressure difference on the cross-section and the focus with respect to the blade center are determined by the formulas

$$\Delta p_s = \rho V_\infty^2 \pi d \frac{\sin\alpha}{4 + \pi \sin\alpha}, \quad \bar{x}_s = \frac{3d}{4} \frac{\cos\alpha}{4 + \pi \sin\alpha}.$$

Computation of Force Factors Acting on the Blade in the Case of Separated Flow

To compute the distributed force factors, i.e., the shearing forces and bending and torsion torques, it is necessary to integrate over the radial coordinate r with integration limits r_1 and r_2.

We introduce the new dimensionless coordinate $\tilde{r} = \omega r/V_0$. The new limits of integration are $\tilde{r}_1 = \omega r_1/V_0$ and $\tilde{r}_2 = \omega r_2/V_0$. In the new variable, the expressions for the trigonometric functions contained in the formulas for the distributed pressures become

$$\sin\alpha = \frac{\omega r}{\sqrt{V_0^2 + \omega^2 r^2}} = \frac{\tilde{r}}{\sqrt{1 + \tilde{r}^2}}, \quad \sin\alpha = \frac{V_0}{\sqrt{V_0^2 + \omega^2 r^2}} = \frac{1}{\sqrt{1 + \tilde{r}^2}}.$$

The gas compressibility in the formulas for the pressure is taken into account by the well-known Prandtl–Glauert corrections [29] $\Delta p_b^c = \Delta p_b/\sqrt{1 - M^2}$ and $\Delta p_s^c = \Delta p_s/\sqrt{1 - M^2}$, where $M = V_0/c$ is the Mach number of the incoming flow.

The flow past rotating blades with the characteristic values of the flow velocity and the rotation angular velocity taken into account occurs with large angle of incidence of the order of 30°–45°, and therefore, we take the flow past blades with separation as the basic scheme. The pressure distribution over the radial coordinate, which follows from the formula for the pressure difference on the plate, has the form

$$q_s(\tilde r) = (1+\tilde r^2)\tilde r/(\pi\tilde r + 4\sqrt{1+\tilde r^2})/\sqrt{1-M^2}.$$

We should integrate this function over $\tilde r$. This can readily be done in the case of flow without separation, but similar formulas for the separated flow and the torque distribution are more complicated and cumbersome, and their integration leads to expressions which can hardly be presented here; see [30].

The distribution of the shear force over the radial coordinate and the total shear force in the root cross-section of the blade become

$$Q_s = \int\limits_{\tilde r}^{\tilde r_2} q_s(\tilde r)\,d\tilde r, \quad Q_\Sigma = \pi\rho V_0^2 d\frac{V_0}{\omega}Q_s(\tilde r_1).$$

The distribution of the bending torque over the radial coordinate and the total bending torque in the blade root cross-section have the form

$$M_s(\tilde r) = \int\limits_{\tilde r}^{\tilde r_2} Q_s(\tilde r)\,d\tilde r, \quad M_\Sigma = \pi\rho V_0^2 d\frac{V_0}{\omega}[M_s(\tilde r_2) - M_s(\tilde r_1)].$$

The distribution of the torque over the radial coordinate is equal to $m_k(\tilde r) = (1+\tilde r^2)\tilde r/(\pi\tilde r + 4\sqrt{1+\tilde r^2})^2/\sqrt{1-M^2}$.

The integral of the distribution over the radial coordinate and the total bending torque are given by the formulas

$$M_k = \int\limits_{\tilde r_1}^{\tilde r_2} m_k(\tilde r)\,d\tilde r, \quad M_{\Sigma k} = \pi\rho V_0^2 d\frac{V_0}{\omega}M_k\frac{3d}{4}.$$

All these total force factors will be used to calculate the additional stresses at the blade root [14, 31].

Computation of Stresses in the Root Cross-Section of the Blade in the Case of Separated Flow

The tangential stresses due to the blade bending and their maximum values, as well as the tangential stresses due to torsion, are determined in the root cross-section by the formulas $\tau_s(y) = Q_\Sigma S_f(y)/(dJ_x)$, $\tau_{s\max} = 3Q_\Sigma/(2dh)$, and $\tau_{sk} = M_{\Sigma k}/(k_s dh^2)$. The normal stresses due to the blade bending and their maximum values in the root cross-section are $\sigma_s(y) = yM_\Sigma/J_x$ and $\sigma_{s\max} = 6M_\Sigma/(dh^2)$.

The computations were performed for the following values of the parameters: $h = 0.015$ m, $d = 0.07$ m, $r_1 = 0.40$ m, $r_2 = 0.70$ m, $V_0 = 220$ m/s, $\omega = 600\ \mathrm{s}^{-1}$, and $\rho = 0.41\ \mathrm{kg/m}^3$.

For these parameters, the additional stresses at the blade root in the case of separated flow are equal to $\tau_{s\max} = 1.3$ MPa, $\sigma_{s\max} = 169$ MPa, and $\tau_{sk} = 0.5$ MPa. The finite-element computations [1, 2] determine the main stress level due to the centrifugal actions as ~ 600–700 MPa for the normal (radial and tangential) stresses and as ~ 50–70 MPa for the circumferential stresses.

In the case of flow without separation, the normal stresses at the blade root take nonrealistic values of the order of 530 MPa, which means that such a scheme of flow past the blades cannot be implemented. More realistic values of aerodynamic loads and related additional stresses on the disk rim are given by the formulas for the flow past blades with separation.

In the scheme of separated flow, the addition tangential stresses, which are of the order of 1/50, i.e., $\sim 2\%$ of the value of the tangential stresses due to the centrifugal loads, can be neglected. The additional normal stresses equal to 170/650, i.e., $\sim 25\%$ of the value of the normal stresses due to the centrifugal loads, should be retained. The influence of the incoming flow is taken into account either additionally, or by using an approximate scheme for taking the aerodynamic loads into account, or directly by solving the coupled gasdynamic–strength problem.

4. COMPUTATION OF THE STRESS-STRAIN STATE OF A ROTATING DISK OF VARIABLE THICKNESS WITH ADDITIONAL AERODYNAMIC LOADS ON THE BLADES TAKEN INTO ACCOUNT

In this section, we solve the problem of determining the stress-strain state of a disk of variable thickness under the action of a periodic system of radial loads produced by the blades on the outer contour.

Derivation of a Simplified System of Differential Equations

In the cylindrical coordinates r, ϑ, z, a ring-shaped disk $0 \le r \le b$ has a variable thickness $-h(r) \le z \le h(r)$. The complete three-dimensional system of elasticity equations in cylindrical coordinates has the form [32]

$$\frac{\partial \sigma_{rr}}{\partial r} + \frac{1}{r}\frac{\partial \sigma_{r\vartheta}}{\partial \vartheta} + \frac{\partial \sigma_{rz}}{\partial z} + \frac{\partial \sigma_{rz}}{\partial z} + \frac{\sigma_{rr} - \sigma_{\vartheta\vartheta}}{r} + \rho\omega^2 r = 0,$$
$$\frac{\partial \sigma_{r\vartheta}}{\partial R} + \frac{1}{r}\frac{\partial \sigma_{\vartheta\vartheta}}{\partial \vartheta} + \frac{\partial \sigma_{\vartheta z}}{\partial z} + \frac{\sigma_{r\vartheta}}{r} = 0,$$
$$\frac{\partial \sigma_{rz}}{\partial r} + \frac{1}{r}\frac{\partial \sigma_{\vartheta z}}{\partial \vartheta} + \frac{\partial \sigma_{zz}}{\partial z} + \frac{\sigma_{rz}}{r}.$$

The stresses are related to Hooke's strain laws as

$$\sigma_{rr} = (\lambda + 2\mu)\varepsilon_{rr} + \lambda\varepsilon_{\vartheta\vartheta} + \lambda\varepsilon_{zz}, \quad \sigma_{\vartheta\vartheta} = \lambda\varepsilon_{rr} + (\lambda + 2\mu)\varepsilon_{\vartheta\vartheta} + \lambda\varepsilon_{zz}, \quad \sigma_{r\vartheta} = 2\mu\varepsilon_{r\vartheta}$$
$$\sigma_{zz} = \lambda\varepsilon_{rr} + \lambda\varepsilon_{\vartheta\vartheta} + (\lambda + 2\mu)\varepsilon_{zz}, \quad \sigma_{rz} = 2\mu\varepsilon_{rz}, \quad \sigma_{\vartheta z} = 2\mu\varepsilon_{\vartheta z}.$$

The strains and displacements are related as

$$\varepsilon_{rr} = \frac{\partial u_r}{\partial r}, \quad \varepsilon_{\vartheta\vartheta} = \frac{1}{r}\frac{\partial u_\vartheta}{\partial \vartheta} + \frac{u_r}{r}, \quad \varepsilon_{r\vartheta} = \frac{1}{2}\left(\frac{1}{r}\frac{\partial u_r}{\partial \vartheta} + \frac{\partial u_\vartheta}{\partial r} - \frac{u_\vartheta}{r}\right),$$
$$\varepsilon_{zz} = \frac{\partial u_z}{\partial z}, \quad \varepsilon_{rz} = \frac{1}{2}\left(\frac{\partial u_r}{\partial z} + \frac{\partial u_z}{\partial z}\right), \quad \varepsilon_{\vartheta z} = \frac{1}{2}\left(\frac{1}{r}\frac{\partial u_z}{\partial \vartheta} + \frac{\partial u_\vartheta}{\partial z}\right).$$

Here λ and μ are the Lamé moduli and ρ is the disk density. In what follows, we use dimensionless stresses referred to $\lambda + 2\mu$ and dimensionless spatial variables referred to the disk radius a.

The boundary conditions on the free surface for $z = \pm h(r)$ have the form $\sigma_{rz} - h'\sigma_{rr} = 0$, $\sigma_{\vartheta z} - h'\sigma_{r\vartheta} = 0$, and $\sigma_{zz} - h'\sigma_{rz} = 0$. The inner contour ($r = a$) is assumed to be stress-free, $\sigma_{rr} = 0$, $\sigma_{r\vartheta} = 0$, and $\sigma_{rz} = 0$. The the outer contour ($r = b$) is subjected to the loads σ_{rr_b} periodic in the circular coordinate ϑ due to centrifugal forces and possibly due to the blade bending under the action of aerodynamic pressures, $\sigma_{rr} = \sigma_{rr\_b}$, $\sigma_{r\theta} = 0$, and $\sigma_{rz} = 0$.

Since all desired functions of the stress-strain state are periodic in the circular coordinate ϑ, we seek the displacements of the ring-shaped disk of variable thickness in the flight loading cycles as the Fourier series

$$u_r = \sum_{n=0}^{\infty}(u_n + u_{2n}z^2 + u_{4n}z^4)\cos(n\vartheta),$$
$$u_\vartheta = \sum_{n=0}^{\infty}(v_n + v_{2n}z^2 + v_{4n}z^4)\cos(n\vartheta),$$
$$u_z = \sum_{n=0}^{\infty}(w_{1n}z + w_{3n}z^3)\cos(n\vartheta).$$

The corresponding representation of stresses has the form

$$\sigma_{rr} = \sum_{n=0}^{\infty}(\sigma_n + \sigma_{2n}z^2)\cos(n\vartheta), \quad \sigma_{\vartheta\vartheta} = \sum_{n=0}^{\infty}(s_n + s_{2n}z^2)\cos(n\vartheta),$$
$$\sigma_{zz} = \sum_{n=0}^{\infty}(\Sigma_n + \Sigma_{2n}z^2 + \Sigma_{4n}z^4)\cos(n\vartheta), \quad \sigma_{r\vartheta} = \sum_{n=0}^{\infty}(\tau_n + \tau_{2n}z^2)\sin(n\vartheta),$$

$$\sigma_{rz} = \sum_{n=0}^{\infty}(p_{1n}z + p_{3n}z^3)\cos(n\vartheta), \quad \sigma_{\vartheta z} = \sum_{n=0}^{\infty}(T_{1n}z + T_{3n}z^3)\sin(n\vartheta).$$

The Fourier coefficients σ_n, τ_n, u_n, v_n are new (auxiliary) desired functions of the radial variable r.

We substitute the expressions for the displacements and stresses into the original system of equilibrium equations and Hooke's law and match the terms with like powers of z up to z^3. As a result, we obtain systems of ordinary differential equations for the auxiliary variables for different $n = 0, 1, 2, \ldots$,

$$\begin{aligned}
&\frac{d\sigma_n}{dr} = -\frac{\sigma_n}{r} + \frac{s_n}{r} - n\frac{\tau_n}{r} - p_{1n},\\
&\frac{d\tau_n}{dr} = -2\frac{\tau_n}{r} + n\frac{s_n}{r} - T_{1n},\\
&\frac{du_n}{dr} = \sigma_n - \lambda\frac{U_n}{r} - \lambda w_{1n},\\
&\frac{dv_n}{dr} = \frac{1}{\mu}\tau_n + \frac{V_n}{r},
\end{aligned} \tag{4.1}$$

where $U_n = nv_n + u_n$, $V_n = nu_n + v_n$, $U_{2n} = nv_{2n} + u_{2n}$, and $V_{2n} = nu_{2n} + v_{2n}$.

This system of equations is solved separately for each harmonic n. The other desired Fourier coefficients u_{2n}, u_{4n}, v_{2n}, v_{4n}, w_{1n}, w_{3n}, σ_{2n}, s_n, s_{2n}, Σ_n, Σ_{2n}, Σ_{4n}, τ_{2n}, p_{1n}, p_{3n}, T_{1n}, and T_{3n} are determined from the auxiliary functions σ_n, τ_n, u_n, v_n by solving the system of ordinary differential equations

$$s_n = \lambda u_n' + \frac{U_n}{r} + \lambda w_{1n}, \quad \Sigma_n = \lambda u_n' + \frac{\lambda U_n}{r} + w_{1n}, \quad w_{1n}' = \frac{p_{1n}}{\mu} - 2u_{2n},$$

$$T_{1n} = \mu\left(2v_{2n} - \frac{nw_{1n}}{r}\right), \quad \sigma_{2n}' = -\frac{\sigma_{2n}}{r} + \frac{s_{2n}}{r} - \frac{n\tau_{2n}}{r} - 3p_{3n}, \quad p_{1n}' = -\frac{p_{1n}}{r} - \frac{nT_{1n}}{r} - 2\Sigma_{2n},$$

$$\tau_{2n}' = -\frac{2\tau_{2n}}{r} + \frac{ns_{2n}}{r} - 3T_{3n}, \quad u_{2n}' = \sigma_{2n} - \frac{\lambda U_{2n}}{r} - 3\lambda w_{3n}, \quad v_{2n}' = \frac{\tau_{2n}}{\mu} + \frac{V_{2n}}{r},$$

$$s_{2n} = \lambda u_{2n}' + \frac{U_{2n}}{r} + 3\lambda w_{3n}, \quad \Sigma_{2n} = \frac{h'^2\sigma_n + h'^2h^2\sigma_{2n} - \Sigma_n - \Sigma_{4n}h^4}{h^2},$$

$$p_{3n} = \frac{h'\sigma_n + h'h^2\sigma_{2n} - p_{1n}h}{h^3}, \quad T_{3n} = \frac{h'\tau_n + h'h^2\tau_{2n} - T_{1n}h}{h^3},$$

$$w_{3n} = \frac{1}{3}\left(\Sigma_{2n} - \lambda u_{2n}' - \frac{\lambda U_{2n}}{r}\right), \quad \Sigma_{4n} = -\frac{1}{4}\left(p_{3n}' + \frac{p_{3n}}{r} + \frac{nT_{3n}}{r}\right),$$

$$u_{4n} = \frac{1}{4}\left(\frac{p_{3n}}{\mu} - w_{3n}'\right), \quad v_{4n} = \frac{1}{4}\left(\frac{T_{3n}}{\mu} + \frac{nw_{3n}}{r}\right).$$

These equations and relations were used in [30] when studying low-cyclic fatigue regimes to solve the problem of determining the stress-strain state and estimating the fatigue life of a rotating disk of variable thickness under the action of centrifugal loads in the disk and blades and under the action of aerodynamic pressures on the blades from the incoming flow.

For $n = 0$, this system coincides with the known equations of axisymmetric deformation of a disk of variable thickness [14] up to the terms containing the factor h'^2.

Boundary Conditions on the Outer Rim of the Disk

To calculate the disk stress-strain state due to the centrifugal loads acting on the blades, the boundary conditions for the auxiliary variables (Fourier coefficients) on the real boundaries $r = a$ and $r = b$ are posed in the form

$$\begin{aligned}
&r = a: \quad \sigma_n = 0, \quad \tau_n = 0,\\
&r = b: \quad \sigma_n = \sigma_{bn}, \quad \tau_n = 0,
\end{aligned} \tag{4.2}$$

where the σ_{bn} are the prescribed values of the Fourier coefficients taking into account the radial stresses on the outer rim of the disk (the stresses in the root cross-sections of the blades under the action of centrifugal loads). To determine σ_{bn}, we assume that the each blade is a plate with rectangular cross-section of width d. The number of blades on the disk is N_0.

The outer contour of the disk is subjected to angle-periodic stresses σ_{rr_b}, which model the centrifugal forces from the blades and are consistent with them in the amplitude, with periodicity sector $-\pi/N_0 < \vartheta < \pi/N_0$,

$$\sigma_{rr\_b} = S_0, \quad |\vartheta| \le \delta.$$

Here $S_0 = \rho\omega^2(b_1^2 - b^2)/2$ is the amplitude of radial stresses determined by the centrifugal action of blades [14], $\delta = d/(2b) \ll 1$, and b and b_1 are the inner and outer radii of blades on the ring-shaped disk.

We expand the periodic radial stress distribution σ_{rr_b} on the outer contour (for $r = b$) in the Fourier series (one period is $-\pi/N_0 < \vartheta < \pi/N_0$)

$$\sigma_{rr\_b} = \sum_n \sigma_{bn} \cos(n\vartheta), \tag{4.3}$$

where $\sigma_{b0} = S_0 N_0 \delta/(2\pi)$ and $\sigma_{bn} = 2S_0 \sin(kN_0\delta/2)/(k\pi)$, $n = 0, N_0, 2N_0, 3N_0, \ldots$

Thus, for various n, one has to solve two-point boundary value problems for a system of ordinary differential equations (4.1) with boundary conditions (4.2) with regard to the expressions (4.3) for the coefficients of the load expansions in the Fourier series in the angular coordinate. These boundary value problems were solved numerically by a finite-element method according to an implicit scheme. After this, the Fourier series were summed to determine the stress components. To obtain practical convergence, it suffices to sum at most 20 terms of the Fourier series.

Taking into Account the Additional Stresses due to the Blade Bending under the Action of Aerodynamic Loads

By analogy with the scheme proposed above, one can compute the additional stresses in the disk due to radial loads on the outer contour caused by the blade bending under the action of aerodynamic pressures. In this case, we assume that the periodic distribution of radial loads on the outer contour for $r = b$ has the form $\sigma_b(\vartheta) = \sigma_{s\max} Y_\delta(\vartheta)$ (one period is $-\pi/N_0 < \vartheta < \pi/N_0$).

Here $\sigma_{s\max} = 6M_\Sigma/(dh^2)$ is the amplitude of radial stresses due to the blade bending under the action of aerodynamics pressures, $Y_\delta(\vartheta) = 2\vartheta/\delta$ for $\vartheta \in [-\delta/2, \delta/2]$, and $Y\delta(\vartheta) = 0$ for $\vartheta \notin [-\delta/2, \delta/2]$. In this case, the Fourier series expansion of the radial load has the form

$$\sigma_b(\vartheta) = \sum_{k=1} \sigma_n \sin(n\vartheta), \quad n = kN_0, \quad \sigma_m = \frac{2}{k\pi}\sigma_{s\max}\left[\frac{\sin(kN_0\delta/2)}{kN_0\delta/2} - \cos\frac{kN_0\delta}{2}\right].$$

For such a loading (antisymmetric with respect to the angular coordinate on the period $-\pi/N_0 < \vartheta < \pi/N_0$), system (4.1) preserves its form after the change $n \to -n$. The solution representation for the stresses differs by the changes $\cos(kN_0\vartheta) \leftrightarrow \sin(kN_0\vartheta)$. In these computations, the rate of convergence of the Fourier series was improved from $1/k$ to $1/k^2$ by "spreading" the discontinuous function $Y_\delta(\vartheta)$ at the points of discontinuity.

Numerical Results

The computations were performed for the disk shape whose cross-section for $z > 0$ is shown in Fig. 3 and for the following parameter values: $N_0 = 32,600\,\mathrm{s}^{-1}$, $\lambda = 78\,\mathrm{MPa}$, $\mu = 44\,\mathrm{MPa}$, and $\rho = 4370\,\mathrm{kg/m}^3$ (titanium alloy). Figure 4 shows the stress component distributions over the radial coordinate for $\vartheta = \vartheta_0 1.074^0$ (the right edge of the blade) and for $z = 0$ without (Figs. 4 *a*, *c*) and with (Figs. 4 *b*, *d*) taking into account the aerodynamic loads on the blades. In Figs. 4 *a*, *b*, the solid line corresponds to the component σ_{rr}, and the dotted line presents the component $\sigma_{r\vartheta}$. In Figs. 4 *c*, *d*, the solid line corresponds to the component $\sigma_{\vartheta\vartheta}$, and the dotted line presents the component σ_{zz}.

These graphs show that if the blade bending due to the aerodynamic pressures is taken into account, then the normal and tangential stresses on the outer rim of the disk increase significantly.

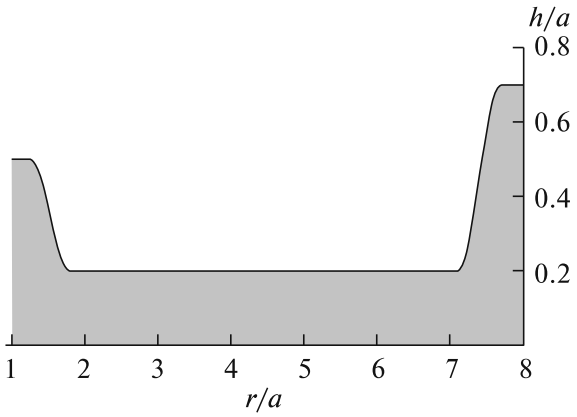

Fig. 3.

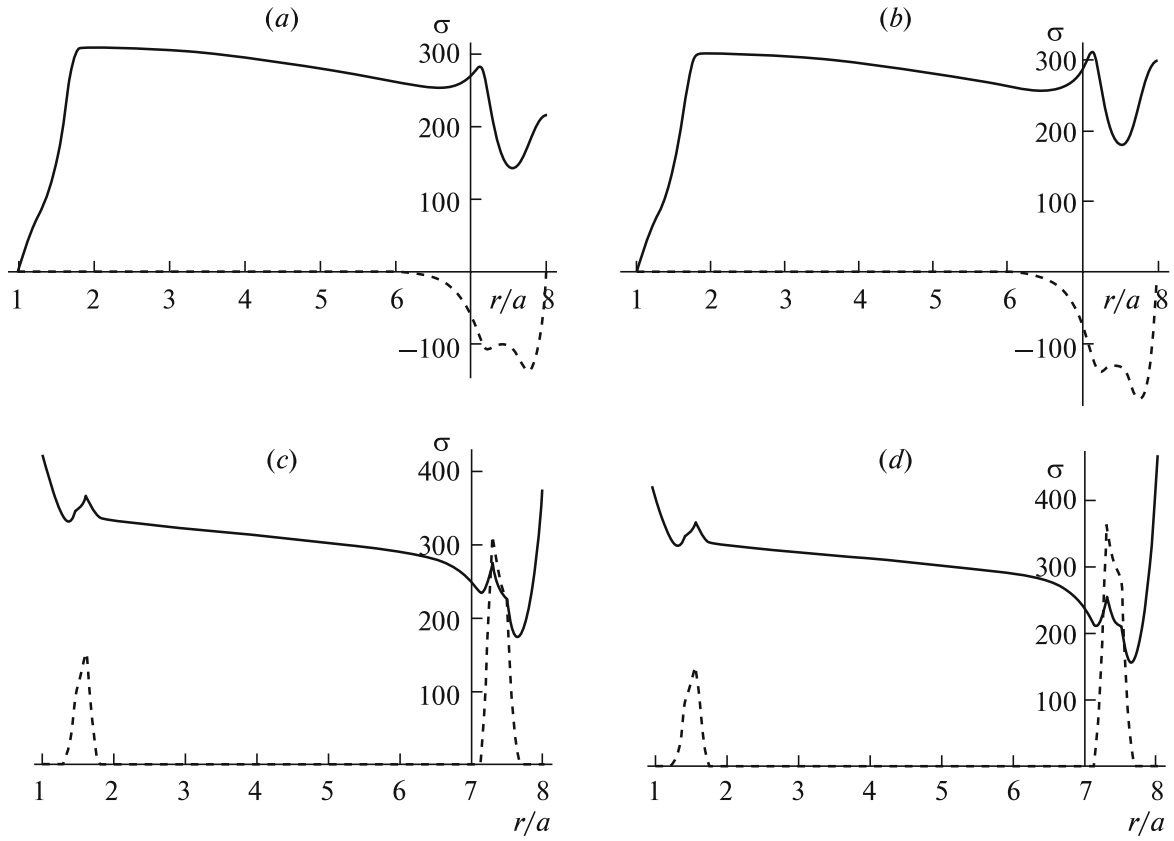

Fig. 4.

Thus, the obtained system (4.1) of ordinary differential equations permitted approximately solving the elasticity problem, which is in fact three-dimensional, and determining the multiaxial stress state of a deformable body with all six nonzero components of the stress tensor with regard to the additional stresses occurring in the rim part of the disk owing to the deformation (bending) of blades under the action of aerodynamic pressures.

Influence of the Anisotropy of the Fatigue Properties on the Disk Lifetime

The criteria for multiaxial fatigue fracture [16] were used to obtain the distributions of the logarithm $\log N(r)$ of the lifetime (the number of loading cycles until fracture) in the radial coordinate for titanium alloy with isotropic fatigue properties and fatigue limit ~ 350 MPa [30]. The Sines criterion was used, and

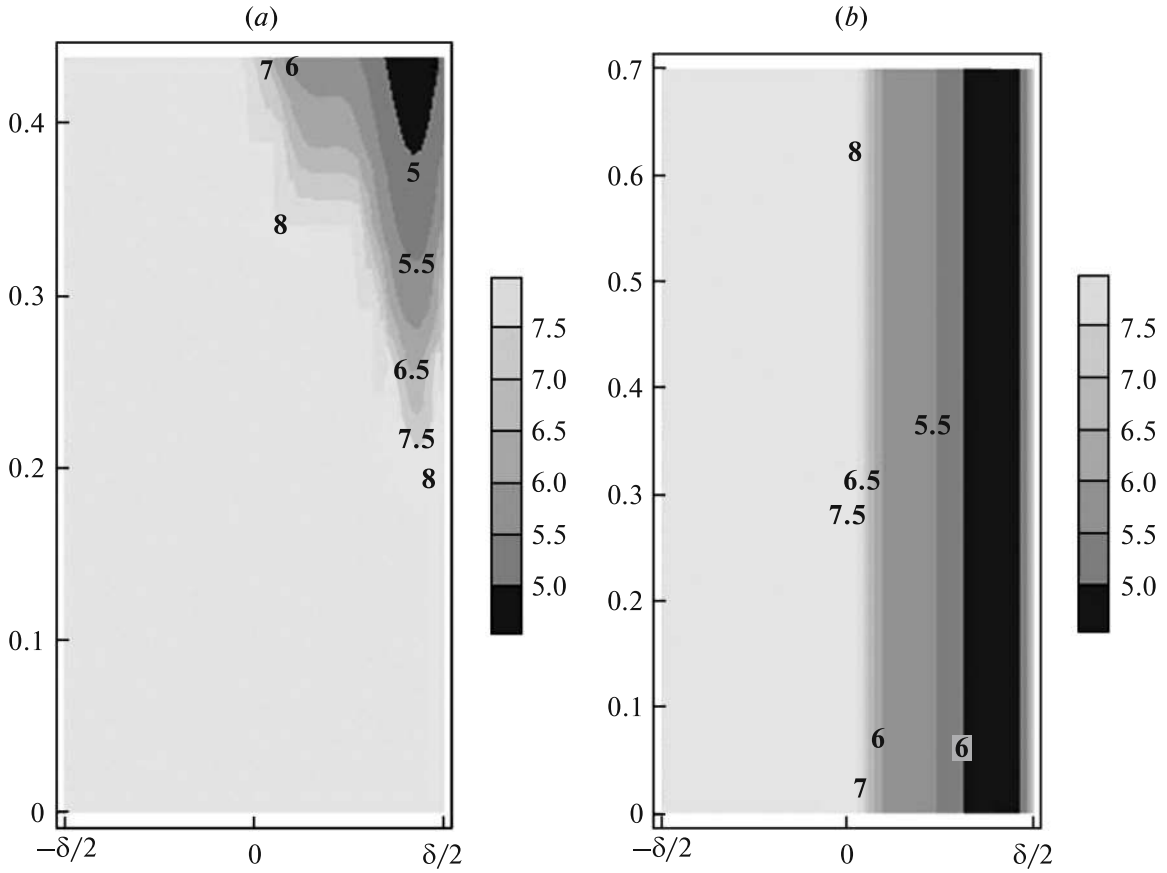

Fig. 5.

the modified Sines criterion was used to compute the fatigue life of a titanium alloy disk with anisotropic fatigue properties. Depending on the blade orientation angle φ with respect to the chosen direction x, the stress component contained in the Hill combination can be computed by the formulas

$$\sigma_{11} = \frac{\sigma_{rr} + \sigma_{\vartheta\vartheta}}{2} + \frac{\sigma_{rr} - \sigma_{\vartheta\vartheta}}{2}\cos(2\varphi) + \sigma_{r\vartheta}\sin(2\varphi),$$
$$\sigma_{22} = \frac{\sigma_{rr} + \sigma_{\vartheta\vartheta}}{2} + \frac{\sigma_{\vartheta\vartheta} - \sigma_{rr}}{2}\cos(2\varphi) - \sigma_{r\vartheta}\sin(2\varphi),$$
$$\sigma_{12} = \frac{\sigma_{\vartheta\vartheta} - \sigma_{rr}}{2}\sin(2\varphi) + \sigma_{r\vartheta}\cos(2\varphi).$$

Lifetime Isoline on Dangerous Cross-Sections for Isotropic and Anisotropic Fatigue

Consider the picture of lifetime distributions in more detail using the isoline graphs in the coordinates z, ϑ in the above-determined dangerous cross-sections under the blade on the outer part of the disk rim for $r = 8$ and in the inner part of the disk for $r = 7.4$. We consider the results obtained for an alloy with isotropic (Fig. 5) and with anisotropic (Fig. 6) fatigue properties for a certain orientation angle φ. The cross-sections under the blades oriented at the angle $\varphi = 90°$ with the anisotropic fatigue axis direction (the rolling direction if we speak about the technological process of the disk manufacturing) are least endurable (Fig. 6: (*a*), inner part of the rim; (*b*), outer part of the rim). The cross-section on the outer rim of the blade for $r = 8$ seems to be most sensitive to the anisotropy of the fatigue properties (Fig. 5 *b* and Fig. 6 *b*).

In these cases, the results are close to each other and take the critical values of the titanium disk fatigue life at the chosen frequencies of rotation of $N \sim 10^4$ cycles, which is inadmissible from the standpoint of safe operation. To avoid this situation, it is required to keep the angular velocities of rotation below the critical values and avoid the technologically induced alloy texture which implies anisotropic fatigue properties.

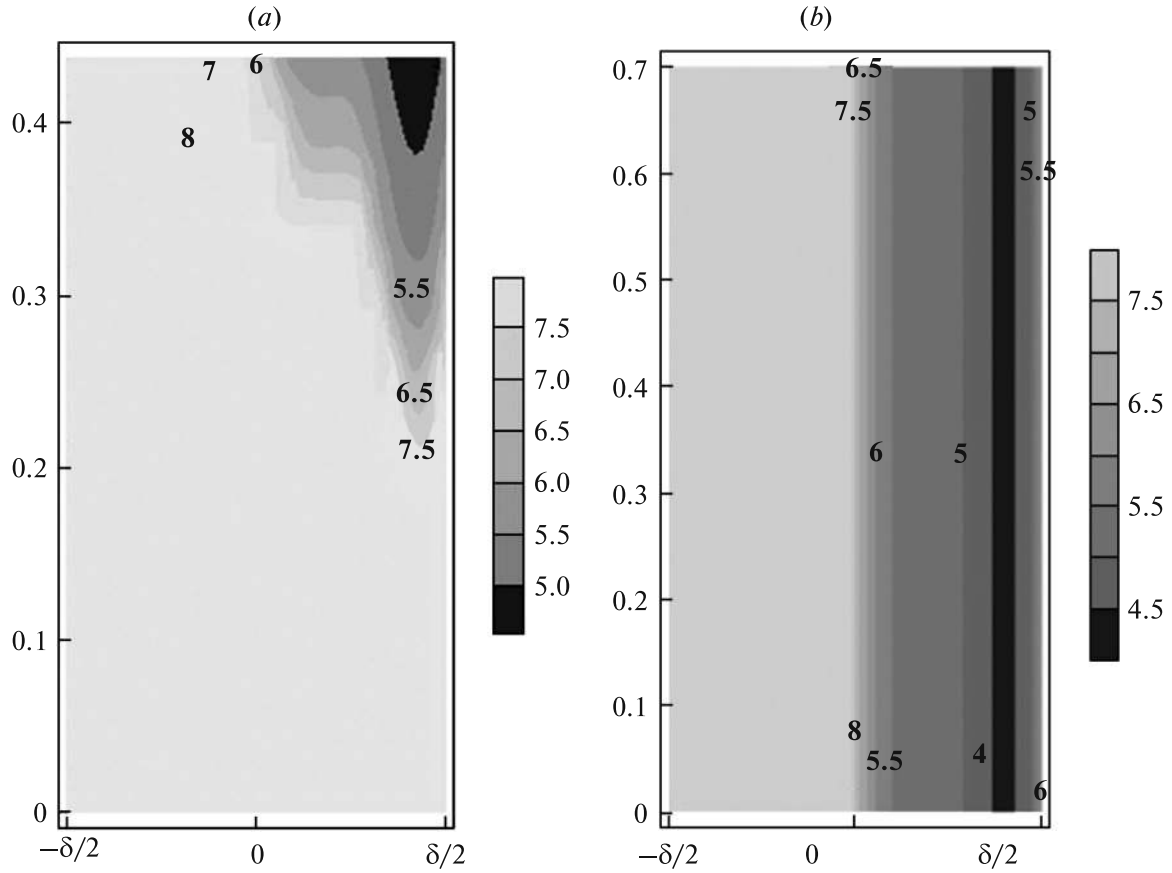

Fig. 6.

5. CONCLUSION

In this paper, we propose a new simplified technique for computing the stress-strain state and lifetime of disks of variable thickness. The technique permits estimating the time constraints ensuring safe operation without large computational costs. The influence of the anisotropy of the fatigue properties due to the technological processes of disk manufacturing is also taken into account and investigated. To this end, the known criteria for multiaxial fracture of isotropic materials are generalized to the case of anisotropic materials. The typical results of lifetime computations are presented for disks of thickness varying along the radius under the conditions of flight cycles of loadings of simplified structure. The regions and time constraints of fatigue fracture origination in the disk are determined. It is shown that the fatigue life of titanium alloys with the anisotropy of the fatigue properties taken into account can decrease to the critical values of $N \sim 10^4$ cycles in the near-surface layers of the disk rims, which is inadmissible from the standpoint of safe operation.

ACKNOWLEDGMENTS

This work was supported by the Russian Foundation for Basic Research, grant No. 15-08-02392-a.

REFERENCES

1. N. G. Burago, A. B. Zhuravlev, and I. S. Nikitin, "Analysis of Stress State of GTE 'Disk-Blade' Contact System," Vych. Mekh. Sploshn. Sred **4** (2), 5–16 (2011).
2. N. N. Beklemishev, N. G. Burago, A. B. Zhuravlev, and I. S. Nikitin, "Aeroelastic Analysis of Structure Elements of a Compressor," Vestnik MAI **18** (5), 3–22 (2011).
3. G. Sines, "Behavior of Metals under Complex Static and Alternating Stress," in *Metal Fatigue* (McGraw-Hill, London, 1958), pp. 145–169.
4. B. Crossland, "Effect of Large Hydrostatic Pressures on Torsional Fatigue Strength of an Alloy Steel," in *Proc. Int. Conf. on Fatigue of Metals* (London, 1956), pp. 138–149.

5. A. Carpinteri, A. Spagnoli, and S. Vantadori, "Multiaxial Assessment Using a Simplified Critical Plane-Based Criterion," Int. J. Fatigue **33**, 969–976 (2011).
6. A. Carpinteri, A. Spagnoli, S. Vantadori, and C. Bagni, "Structural Integrity Assessment of Metallic Components under Multiaxial Fatigue: The C-S Criterion and Its Evolution," Fatigue Fract. Engng Mater. Struct. **36**, 870–883 (2013).
7. L. Susmel and D. Taylor, "A Critical Distance/Plane Method to Estimate Finite Life of Notched Components under Variable Amplitude Uniaxial/Multiaxial Fatigue Loading," Int. J. Fatigue **38**, 7–24 (2012).
8. W. Findley, "A Theory for the Effect of Mean Stress on Fatigue of Metals under Combined Torsion and Axial Load or Bending," J. Engng Indust., 301–306 (2959).
9. N. G. Burago, I. S. Nikitin, A. A. Shanyavskii, and A. B. Zhuravlev, "Durability Estimations for In-Service Titanium Compressor Disks to Multiaxial Cyclic Loads in Low- and Very-High-cyclic Fatigue Regimes," in *Proc. 19th European Conference on Fracture, Kazan 26–31 August 2012*, (CD ver.), Auth. Ind. 154.
10. R. Hill, *The Mathematical Theory of Plasticity* (Clarendon Press, Oxford, 1950; Gostekhizdat, Moscow, 1956) [in Russian].
11. D. V. Toporov, B. V. Ilchenko, and R. R. Yarulin, "Characteristics of Static and Low-Cyclic Strength of Critical Zones of Turbine Disk," Trudy Akademenergo, No. 2, 79–88 (2010).
12. V. N. Shlyannikov, R. R. Yarullin, and R. Z. Gizzatullin, "Structural Integrity Prediction of Turbine Disk on a Critical Zone Concept Basis," in *Proc. 11th International Conference on Engineering Structural Integrity Assessment. ESIA11, Manchester UK* (EMAS Publ. 2011), pp. 1–10.
13. B. V. Ilchenko, R. R. Yarulin, A. P. Zakharov, and R. Z. Gizzatullin, "Residual Life Prediction of Power Steam Turbine Disk with Fixed Operating Time," in *Proc. 19th European Conference on Fracture, ECG19, Kazan, Russia, 26–31 August 2012*, (Kazan', 2012) pp. 1–8.
14. I. V. Dem'yanushko and I. A. Birger, *Strength Computation of Rotating Disks* (Mashinostroenie, Moscow, 1978) [in Russian].
15. N. G. Burago, A. B. Zhuravlev, and I. S. Nikitin, "Superpower Cyclic Fatigue Fracture of Compressor Titanium Disks," Vetnik PNIPU, Mekhanika, No. 1, 52–67 (2013).
16. N. G. Bourago, A. B. Zhuravlev, and I. S. Nikitin, "Models of Multiaxial Fatigue Fracture and Service Life Estimation of Structural Elements," Izv. Akad. Nauk. Mekh. Tverd. Tela, No. 6, 22–33 (2011) [Mech. Solids (Engl. Transl.) **46** (6), 828–838 (2011)].
17. A. A. Shanyavskii, *Modeling of Metal Fatigue fracture* (OOO "Monografiya", Ufa, 2007) [in Russian].
18. A. A. Il'in, B. A. Kolachev, and I. S. Pol'kin, *Titanium Alloys, Composition, Structure, Properties* (VILS-MATI, Moscow, 2009) [in Russian].
19. I. V. Gorynin and B. B. Chechulin, *Titanium in Engineering Industry* (Mashinostroenie, Moscow, 1990) [in Russian].
20. A. Sommer, M. Kriger, S. Fudzisiro, and D. Eilon, "Texture Development in $\alpha + \beta$-Titanium Alloys," in *Titanium. Physical Metallurgy and Technology. Proc. 3rd Intern. Conf. on Titanium*, Vol. 3 (VILS, Moscow, 1978), pp. 87–96 [in Russian].
21. A. K. Marmi, A. M. Habraken, and L. Duchene, "Multiaxial Fatigue Damage Modeling at Marco Scale of Ti6Al4V Alloy," Int. J. Fatigue **31**, 2031–2040 (2009).
22. A. K. Marmi, A. M. Habraken, and L. Duchene, "Multiaxial Fatigue Damage Modeling of Ti6Al4V Alloy," in *Proc. 9th Int. Conf. on Multiaxial Fatigue and Fracture (ICMFF9), Parma, Italy, 2010* (Parma, 2010), pp. 559–567.
23. I. A. Birger and Ya. G. Panovko (Editors), *Strength. Stability. Oscillations*, Vol. 1 (Mashinostroenie, Moscow, 1990) [in Russian].
24. I. A. Birger, *Beams, Plane, and Shells* (Fitmatlit, Moscow, 1992) [in Russian].
25. A. G. Kostyuk, *Dynamics and Turbomachine Strength* (Izdat. Dom MEI, Moscow, 2007) [in Russian].
26. A. A. Inozemtsev, M. A. Nikhamkin, V. L. Sandratskii, *Dynamic and Strength of Aircraft Engines and Power Plants* (Mashinostroenie, Moscow, 2008) [in Russian].
27. A. M. Mkhitaryan, *Aerodynamics* (Mashinostroenie, Moscow, 1976) [in Russian].
28. N. E. Kochin, I. A. Kibel', N. V. Roze, *Theoretical Hydromechanics*, Part 1 (Fizmatgiz, Moscow, 1963) [in Russian].
29. M. I. Gurevich, *Theory of Perfect Liquid Jets* (Nauka, Moscow, 1979) [in Russian].
30. N. G. Burago, A. B. Zhuravlev, I. S. Nikitin, and P. A. Yushkovskii, *Influence of Anisotropy of Fatigue Properties of a Titanium Alloy on Lifetime of Structural Elements*, Preprint No. 1064 (IPMekh RAN, Moscow, 2014) [in Russian].
31. Yu. N. Rabotnov, *Mechanics of Deformable Solids* (Nauka, Moscow, 1979) [in Russian].
32. W. Nowacki, *Theory of Elasticity* (PWN, Warszawa, 1970; Mir, Moscow, 1975).
33. V. N. Kukudzhanov, *Computational Mechanics of Continua* (Fizmatlit, Moscow, 2006) [in Russian].